AIMS *Mathematics*

https://www.aimspress.com/journal/Math

AIMS Mathematics, 11(8): 24667–24690.
DOI: 10.3934/math.2026993
Received: 29 April 2026
Revised: 03 July 2026
Accepted: 22 July 2026
Published: 12 August 2026

Research article

Bayesian inference of double seasonal autoregressive models under scale-mixtures of normal errors with applications

Ayman A. Amin[1,2] and Farouq Mohammad A. Alam[3,*]

[1] Department of Mathematics, College of Science and Arts, Najran University, Najran, Saudi Arabia

[2] Science and Engineering Research Center, Najran University, Najran, Saudi Arabia

[3] Department of Statistics, Faculty of Science, King Abdulaziz University, Jeddah 21589, Saudi Arabia

* **Correspondence:** Email: fmalam@kau.edu.sa.

Abstract: Double seasonal autoregressive (DSAR) models have been developed for modeling time series characterized by two layers of seasonal behavior. A prevalent limitation in existing Bayesian analysis of these models is their reliance on the Gaussian errors assumption, which is routinely violated by empirical data. To overcome this restriction, we develop a Bayesian inferential framework for DSAR models in which the error term is governed by the scale-mixtures of normal (SMN) family, which is a flexible class of symmetric, heavy-tailed distributions. By assigning carefully chosen prior distributions to the DSAR parameters, we establish closed-form full conditional posteriors, i.e., a multivariate normal for the DSAR coefficient vectors and an inverse-gamma for the scale parameter. The conditional posteriors associated with the SMN-specific parameters are likewise obtained in closed form, although certain members of this collection do not correspond to standard distributional families. Exploiting these tractable conditional posteriors, we construct a hybrid Markov chain Monte Carlo (MCMC) algorithm—the Gibbs sampler interlaced with Metropolis-Hastings steps—to approximate the marginal posterior distributions of all DSAR parameters. The performance of the proposed algorithm is assessed through an extensive Monte Carlo simulation experiment and through real-data analyses of hourly electricity load records in Croatia and Italy.

Keywords: multiplicative DSAR; posterior analysis; MCMC methods; Gibbs sampler; metropolis-Hastings
Mathematics Subject Classification: 37M10, 62F15

1. Introduction

Even for the simplest seasonal structure, the Bayesian treatment of seasonal autoregressive (SAR) models poses substantial analytical challenges, primarily because the likelihood function is nonlinear in the model coefficients, rendering the associated posterior densities unavailable in closed form [1]. Two broad strategies have emerged in the Bayesian time series literature to cope with this intractability: analytical approximation schemes and simulation-based approaches rooted in Markov chain Monte Carlo (MCMC) methodology [2].

Analytical approximations seek to render the posterior density expressible in standard form. Research in this vein dates back to Shaarawy and Ismail [3] and extends to more recent contributions such as Amin and Alghamdi [4]. A notable shortcoming shared by these methods is that they handle seasonal models additively rather than multiplicatively, artificially inflating the model dimension with redundant parameters. The adoption of MCMC techniques, and the Gibbs sampler in particular, represents a more principled and scalable approach for approximating the posterior distributions of multiplicative seasonal models.

MCMC-based posterior analysis of SAR models under Gaussian errors was pioneered by Barnett et al. [5, 6], who employed partial-autocorrelation sampling functions to handle multiplicative SAR and autoregressive moving average (ARMA) specifications. For speech modeling applications, Vermaak et al. [7] cast SAR models in state-space form and employed a Gibbs–Metropolis sampler for Bayesian estimation. Ismail and Amin [8] formally introduced Gibbs sampling for mixed seasonal ARMA models; and this line was further advanced by Amin [9], who incorporated predictive inference.

Research addressing Bayesian analysis of multiple layers of seasonality remains comparatively sparse. Amin and Ismail [10] developed Gibbs-sampler-based Bayesian estimators for DSAR models under the assumption of Gaussian errors. Complementary work by Amin [11, 2] established Bayesian predictive and fully inferential procedures for double seasonal autoregressive (DSAR) models.

A separate stream of research has introduced non-Gaussian error distributions into Bayesian AR modeling, though typically without accommodating a double seasonal structure. Ferreira et al. [12] considered partial linear models with first-order AR residuals following the scale-mixtures of normal (SMN) distribution; Mahmoudi et al. [13] studied heavy-tailed finite mixtures of AR models; Ryu and Kim [14] adopted the exponential power family for AR errors; and Agarwal and Tripathi [15] proposed a Bayesian treatment of AR models driven by a nonstandardized Student's t distribution. Amin and Alghamdi [16] proposed an MCMC algorithm under the SMN distribution for the Bayesian estimation of AR models with exogenous variables. Recently, Amin [17, 18] introduced MCMC procedures under the SMN distribution for the Bayesian predictive and fully inferential analysis of SAR models, underscoring the practical relevance of this distributional framework for seasonal time series.

Drawing on these motivations, the present paper addresses a gap at the intersection of doubly seasonal time series modeling and robust Bayesian inference. We introduce a comprehensive Bayesian framework for DSAR models, assuming the errors follow the SMN distribution, and we develop a Gibbs sampler augmented with Metropolis-Hastings steps for posterior inference. The SMN family constitutes a broad, flexible class of symmetric distributions encompassing several heavy-tailed members as particular instances, including the Student's t, slash, and contaminated normal distributions [19, 20]. Under alternative prior specifications for the DSAR parameters, we derive closed-form full conditional posteriors for the DSAR coefficient vectors and the scale parameter. Although we derive the conditional posteriors for the SMN-specific parameters in closed form, some of them are nonstandard and therefore require Metropolis-Hastings transitions. The resulting algorithm is validated on synthetic data and applied to hourly electricity load series from Croatia and Italy.

The remainder of the paper is organized as follows. Section 2 reviews the SMN distribution and defines the DSAR model class. Section 3 develops the joint likelihood and prior structure and formulates the posterior analysis. Section 4 derives the full conditional distributions and presents the proposed MCMC algorithm. Section 5 reports the simulation study and the real-data applications. Section 6 concludes the work.

2. DSAR models with scale-mixtures of normal errors

This section introduces the SMN distributional family and defines the class of DSAR models considered throughout the paper.

2.1. Scale-Mixtures of normal distribution

The SMN family provides a versatile and mathematically elegant class of symmetric, heavy-tailed probability distributions. It encompasses many well-known distributions as special cases, including the Student's t, Cauchy, slash, and contaminated normal, as well as the Gaussian distribution itself [19, 20]. The theoretical attractiveness of this family lies in its hierarchical construction. A random variable belonging to the SMN class can always be expressed as a location-scale mixture of Gaussian variates, where the scale factor follows some nonnegative mixing distribution. This representation not only unifies a diverse set of models within a single coherent framework but also facilitates efficient MCMC-based inference through data augmentation [21].

The SMN representation further provides a principled mechanism for accommodating outliers and departures from normality that frequently appear in real data, including time series of electricity demand, financial returns, and environmental measurements. When the mixing variable u has high probability mass near zero, the resulting marginal distribution exhibits heavier tails than the Gaussian, increasing the model's robustness to extreme observations. Conversely, when u concentrates its mass near one, the SMN distribution approaches the Gaussian, making the latter a limiting case that is automatically handled within the same inferential framework.

Formal Definition. A random variable y is said to follow an SMN distribution with location μ and scale σ^2 if it admits the stochastic representation:

$$y \;=\; \mu + u^{-1/2}\varepsilon, \tag{2.1}$$

where $\varepsilon \sim N(0, \sigma^2)$ independently of the positive mixing variable u, which has density $p(u \mid \boldsymbol{\nu})$ parameterized by a scalar or vector $\boldsymbol{\nu}$ [20]. Marginally over u, the variable $y \mid \mu, \sigma^2, \boldsymbol{\nu}$ has a heavier-tailed distribution than the normal distribution, and the specific shape is governed entirely by the choice of mixing density.

Special Cases. The following distributions are recovered as special cases of the SMN representation (2.1), which is a key practical advantage of the framework:

1. *Student's t (SMN-t):* When $u \sim G(\nu/2, \nu/2)$ with $\nu > 0$, the marginal distribution of y is a Student's t with ν degrees of freedom. The parameter ν controls tail heaviness. Small values of ν yield heavy tails (Cauchy when $\nu = 1$), while $\nu \to \infty$ recovers the Gaussian [22].
2. *Slash (SMN-sl):* When $u \sim \text{Beta}(\nu, 1)$ with $\nu > 0$, the resulting marginal is the slash distribution. The slash distribution has polynomial tail decay and is, therefore, heavier-tailed than the Student's t for any fixed ν [23].
3. *Contaminated Normal (SMN-cn):* When u is discrete, taking the value $\gamma \in (0, 1)$ with probability $\nu \in (0, 1)$ and the value 1 with probability $1 - \nu$, i.e.,

$$p(u \mid \nu, \gamma) \;=\; \nu \mathbb{I}_{\{\gamma\}}(u) + (1 - \nu)\mathbb{I}_{\{1\}}(u), \quad \nu, \gamma \in (0, 1), \tag{2.2}$$

   the marginal is the contaminated normal, a mixture of two Gaussian components sharing the same mean but with different variances. Here, $\mathbb{I}_{\{a\}}(u)$ denotes the indicator function, equal to 1 if $u = a$ and 0 otherwise. It provides a natural model for data subject to occasional outliers generated by an inflated-variance mechanism [24].
4. *Normal (SMN-n):* The degenerate case $p(u = 1) = 1$ yields the standard Gaussian, confirming that the normal distribution is nested within the SMN family.

Table 1 summarizes the mixing distributions and the resulting SMN special cases for convenient reference.

Table 1. Summary of special cases of the SMN distribution.

SMN Case	Mixing distribution $p(u \mid \nu)$	Parameter constraints
SMN-t	$u \sim G(\nu/2,\ \nu/2)$	$\nu > 0$
SMN-sl	$u \sim \text{Beta}(\nu, 1)$	$\nu > 0$
SMN-cn	$p(u) = \nu\, \mathbb{I}_{\{\gamma\}}(u) + (1 - \nu)\, \mathbb{I}_{\{1\}}(u)$	$\nu, \gamma \in (0, 1)$
SMN-n	$p(u = 1) = 1$	—

The hierarchical structure of the SMN representation is also computationally advantageous. Thus, by treating the latent weights $u_1, \ldots, u_n$ as auxiliary variables, one can derive tractable full conditional distributions for all model parameters, enabling efficient Gibbs sampling [21, 25]. This data-augmentation strategy is a cornerstone of the MCMC algorithm developed in Section 4.

2.2. DSAR models

A time series $\{y_t\}$ is said to obey a multiplicative double seasonal autoregressive model of orders p_1, p_2, and p_3—denoted $\text{DSAR}(p_1)(p_2)_{s_1}(p_3)_{s_2}$—if it satisfies [2]:

$$\boldsymbol{\phi}_\mathbf{1}(B)\, \boldsymbol{\phi}_\mathbf{2}(B^{s_1})\, \boldsymbol{\phi}_\mathbf{3}(B^{s_2})\, y_t = \varepsilon_t, \tag{2.3}$$

where the innovations ε_t are a zero-mean sequence with scale σ^2; B denotes the back-shift operator satisfying $B^r z_t = z_{t-r}$; and s_1, s_2 are the two known seasonal periods. In this paper, we specify ε_t to follow the SMN family (Section 2.1), enabling DSAR models to accommodate heavy-tailed and outlier-contaminated data; the general DSAR model class does not presuppose this particular distributional form.

The autoregressive polynomials are defined as: $\boldsymbol{\phi_1}(B) = 1-\phi_{11}B-\phi_{12}B^2-\cdots-\phi_{1p_1}B^{p_1}$ (nonseasonal component of order p_1); $\boldsymbol{\phi_2}(B^{s_1}) = 1-\phi_{21}B^{s_1}-\phi_{22}B^{2s_1}-\cdots-\phi_{2p_2}B^{p_2s_1}$ (first seasonal component of order p_2); and $\boldsymbol{\phi_3}(B^{s_2}) = 1-\phi_{31}B^{s_2}-\phi_{32}B^{2s_2}-\cdots-\phi_{3p_3}B^{p_3s_2}$ (second seasonal component of order p_3). The corresponding coefficient vectors are $\boldsymbol{\phi_1} = (\phi_{11},\ldots,\phi_{1p_1})^T$, $\boldsymbol{\phi_2} = (\phi_{21},\ldots,\phi_{2p_2})^T$, and $\boldsymbol{\phi_3} = (\phi_{31},\ldots,\phi_{3p_3})^T$. Throughout the paper, the i-th coefficient vector is denoted $\boldsymbol{\phi_i}$ and the remaining two are collectively written as $\boldsymbol{\phi_{(-i)}}$.

Expanding the operator product in (2.3) yields the explicit regression form:

$$\begin{aligned} y_t &= \sum_{i=1}^{p_1}\phi_{1i}y_{t-i}+\sum_{j=1}^{p_2}\phi_{2j}y_{t-js_1}+\sum_{l=1}^{p_3}\phi_{3l}y_{t-ls_2}-\sum_{i=1}^{p_1}\sum_{j=1}^{p_2}\phi_{1i}\phi_{2j}y_{t-i-js_1}- \\ &\quad \sum_{i=1}^{p_1}\sum_{l=1}^{p_3}\phi_{1i}\phi_{3l}y_{t-i-ls_2}-\sum_{j=1}^{p_2}\sum_{l=1}^{p_3}\phi_{2j}\phi_{3l}y_{t-js_1-ls_2}+ \\ &\quad \sum_{i=1}^{p_1}\sum_{j=1}^{p_2}\sum_{l=1}^{p_3}\phi_{1i}\phi_{2j}\phi_{3l}y_{t-i-js_1-ls_2}+\varepsilon_t \\ &= \boldsymbol{x}_t^T\boldsymbol{\beta}+\varepsilon_t, \end{aligned} \tag{2.4}$$

where the regressor vector $\boldsymbol{x}_t$ is given by:

$$\begin{aligned} \boldsymbol{x}_t &= \big(y_{t-1},\ldots,y_{t-p_1},y_{t-s_1},y_{t-s_1-1},\ldots,y_{t-s_1-p_1},\ldots\ldots,y_{t-p_2s_1},y_{t-p_2s_1-1},\ldots, \\ &\quad y_{t-p_2s_1-p_1},y_{t-s_2},y_{t-s_2-1},\ldots,y_{t-s_2-p_1},y_{t-s_1-s_2},y_{t-s_1-s_2-1},\ldots,y_{t-s_1-s_2-p_1}, \\ &\quad \ldots\ldots,y_{t-p_2s_1-s_2},y_{t-p_2s_1-s_2-1},\ldots,y_{t-p_2s_1-s_2-p_1},\ldots\ldots\ldots,y_{t-p_3s_2},y_{t-p_3s_2-1}, \\ &\quad \ldots,y_{t-p_3s_2-p_1},y_{t-s_1-p_3s_2},y_{t-s_1-p_3s_2-1},\ldots,y_{t-s_1-p_3s_2-p_1},\ldots\ldots, \\ &\quad y_{t-p_2s_1-p_3s_2},y_{t-p_2s_1-p_3s_2-1},\ldots,y_{t-p_2s_1-p_3s_2-p_1}\big), \end{aligned} \tag{2.5}$$

and the generalized coefficient vector $\boldsymbol{\beta}$, whose elements include all products of the three sets of autoregressive coefficients, is:

$$\begin{aligned} \boldsymbol{\beta} &= \big(\phi_{11},\ldots,\phi_{1p_1},\phi_{21},-\phi_{11}\phi_{21},\ldots,-\phi_{1p_1}\phi_{21},\ldots\ldots,\phi_{2p_2},-\phi_{11}\phi_{2p_2},\ldots,-\phi_{1p_1}\phi_{2p_2}, \\ &\quad \phi_{31},-\phi_{11}\phi_{31},\ldots,-\phi_{1p_1}\phi_{31},-\phi_{21}\phi_{31},\phi_{11}\phi_{21}\phi_{31},\ldots,\phi_{1p_1}\phi_{21}\phi_{31},\ldots\ldots,-\phi_{2p_2}\phi_{31}, \\ &\quad \phi_{11}\phi_{2p_2}\phi_{31},\ldots,\phi_{1p_1}\phi_{2p_2}\phi_{31},\ldots\ldots\ldots,\phi_{3p_3},-\phi_{11}\phi_{3p_3},\ldots,-\phi_{1p_1}\phi_{3p_3},-\phi_{21}\phi_{3p_3}, \\ &\quad \phi_{11}\phi_{21}\phi_{3p_3},\ldots,\phi_{1p_1}\phi_{21}\phi_{3p_3},\ldots\ldots,-\phi_{2p_2}\phi_{3p_3},\phi_{11}\phi_{2p_2}\phi_{3p_3},\ldots,\phi_{1p_1}\phi_{2p_2}\phi_{3p_3}\big)^T. \end{aligned} \tag{2.6}$$

To facilitate the subsequent Bayesian derivations, we collect all n observations into the compact matrix representation:

$$\boldsymbol{y} = \boldsymbol{X}\boldsymbol{\beta}+\boldsymbol{\varepsilon}, \tag{2.7}$$

where $\boldsymbol{y} = (y_1,\ldots,y_n)^T$, $\boldsymbol{\varepsilon} = (\varepsilon_1,\ldots,\varepsilon_n)^T$, and $\boldsymbol{X}$ is the $n\times m$ design matrix with $m = (1+p_1)(1+p_2)(1+p_3)-1$ and t-th row $\boldsymbol{x}_t$ as defined in (2.5).

A critical observation from (2.6) is that $\boldsymbol{\beta}$ contains cross-products of the primitive coefficients, e.g., $\phi_{1i}\phi_{2j}$. This multiplicative structure renders the DSAR model inherently nonlinear in $\boldsymbol{\phi_1}$, $\boldsymbol{\phi_2}$, and $\boldsymbol{\phi_3}$, which substantially complicates the Bayesian analysis, as detailed in subsequent sections.

3. Posterior analysis of DSAR models with SMN errors

Given the SMN distributional assumption on the DSAR errors introduced in Section 2, the marginal density of the observed time series $\boldsymbol{y}$ can be expressed as:

$$\begin{aligned}\zeta(\boldsymbol{y} \mid \boldsymbol{\phi}_i' s, \sigma^2) &= \prod_{t=1}^{n} \int p(y_t|\boldsymbol{\phi}_i' s, \sigma^2, u_t) p(u_t|\boldsymbol{\nu}) du_t \\ &\propto \prod_{t=1}^{n} \int \left\{u_t^{1/2} p(u_t|\boldsymbol{\nu})\right\} \times \\ & \quad (\sigma^2)^{-\frac{n}{2}} \exp\left\{-\frac{u_t}{2\sigma^2}\left(y_t - \boldsymbol{x}_t^T \boldsymbol{\beta}\right)^2\right\} du_t. \end{aligned} \tag{3.1}$$

Directly working with this integrated likelihood is cumbersome. Following the data-augmentation strategy [21], we introduce the latent weight vector $\boldsymbol{u} = (u_1, \ldots, u_n)^T$ and work with the complete-data joint density:

$$\begin{aligned}\zeta(\boldsymbol{y}, \boldsymbol{u} \mid \boldsymbol{\phi}_i' s, \sigma^2, \boldsymbol{\nu}) &\propto \prod_{t=1}^{n} \left\{u_t^{1/2} p(u_t|\boldsymbol{\nu})\right\} \times \\ & \quad (\sigma^2)^{-\frac{n}{2}} \exp\left\{-\frac{1}{2\sigma^2} \sum_{t=1}^{n} u_t \left(y_t - \boldsymbol{x}_t^T \boldsymbol{\beta}\right)^2\right\}, \end{aligned} \tag{3.2}$$

where $p(u_t \mid \boldsymbol{\nu})$ is the mixing density appropriate to the chosen SMN case, as described in Section 2.1.

Prior specification. Let $\Theta = (\boldsymbol{\phi}_1, \boldsymbol{\phi}_2, \boldsymbol{\phi}_3, \sigma^2, \boldsymbol{\nu})$ denote the full parameter vector. We assume prior independence between $(\boldsymbol{\phi}_i' s, \sigma^2)$ and $\boldsymbol{\nu}$, so the joint prior factorizes as:

$$\zeta(\Theta|\boldsymbol{H}) = \zeta(\boldsymbol{\phi}_i' s, \sigma^2|\boldsymbol{H}_1) \times \zeta(\boldsymbol{\nu}|\boldsymbol{H}_2), \tag{3.3}$$

where $\boldsymbol{H}$, $\boldsymbol{H}_1$, and $\boldsymbol{H}_2$ are collections of hyperparameters, and $\zeta(\boldsymbol{\phi}_i' s, \sigma^2 \mid \boldsymbol{H}_1)$ may be specified as a normal-gamma, g, or Jeffreys' prior.

Normal-gamma prior. Conditional on σ^2 and assuming mutual prior independence across i:

$$\begin{aligned}\zeta(\boldsymbol{\phi}_i' s, \sigma^2|\boldsymbol{H}_1) &= \prod_{i=1}^{3} \zeta(\boldsymbol{\phi}_i|\sigma^2) \times \zeta(\sigma^2) \\ &= \prod_{i=1}^{3} N_{p_i}(\boldsymbol{\mu}_{\boldsymbol{\phi}_i}, \sigma^2 \boldsymbol{\Sigma}_{\boldsymbol{\phi}_i}) \times IG\left(\frac{a_0}{2}, \frac{b_0}{2}\right), \end{aligned} \tag{3.4}$$

where $N_r(\boldsymbol{\mu}, \boldsymbol{\Delta})$ denotes an r-variate normal with mean $\boldsymbol{\mu}$ and covariance $\boldsymbol{\Delta}$, and $IG(a, b)$ is the inverse-gamma with shape a and rate b. Combining the three normal components yields the joint normal-gamma prior:

$$\zeta(\boldsymbol{\phi}_i' s, \sigma^2|\boldsymbol{H}_1) \propto (\sigma^2)^{-\left(\frac{a_0+p_1+p_2+p_3}{2}+1\right)} \exp\left\{-\frac{1}{2\sigma^2}\left[b_0 + \sum_{i=1}^{3}\left(\boldsymbol{\phi}_i - \boldsymbol{\mu}_{\boldsymbol{\phi}_i}\right)^T \times\right.\right.$$

$$\Sigma_{\phi_i}^{-1}\left(\phi_i - \mu_{\phi_i}\right)\Big]\Big\}. \tag{3.5}$$

g **prior.** When eliciting a full covariance structure is impractical, Zellner's g prior [26] offers a parsimonious alternative:

$$\zeta(\phi_i's, \sigma^2|\boldsymbol{H}_1) \quad \propto \quad (\sigma^2)^{-(\frac{m}{2}+1)} \exp\left\{-\frac{g}{2\sigma^2}\left(\boldsymbol{\beta}-\bar{\boldsymbol{\beta}}\right)^T (\boldsymbol{X}^T\boldsymbol{X})\left(\boldsymbol{\beta}-\bar{\boldsymbol{\beta}}\right)\right\}, \tag{3.6}$$

where $\bar{\boldsymbol{\beta}}$ is a prior expectation for $\boldsymbol{\beta}$, and the scalar hyperparameter g is typically calibrated to the sample size, e.g., $g = n^{-1}$; see Fernandez et al. [27] and Amin [28] for further discussion.

Jeffreys' prior. In the absence of reliable prior information, one may adopt the scale-invariant Jeffreys' prior [29]:

$$\zeta\left(\phi_i's, \sigma^2\right) \quad \propto \quad (\sigma^2)^{-1}, \quad \sigma^2 > 0. \tag{3.7}$$

The prior for the SMN-specific parameter $\boldsymbol{\nu}$ depends on the distributional case. Following the conjugacy-guided recommendations of Cabral et al. [30], we specify the following case-by-case priors. For SMN-t, ν is assigned a truncated exponential distribution with rate $\lambda > 0$, restricted to $(2, \infty)$, with λ itself given a uniform prior on (c, d). For SMN-sl, the same exponential structure applies but with support $(1, \infty)$. For SMN-cn, ν and γ independently receive beta priors: $\nu \sim \text{Beta}(\nu_0, \nu_1)$ and $\gamma \sim \text{Beta}(\gamma_0, \gamma_1)$, with positive hyperparameters.

Joint posterior. Combining the complete-data likelihood (3.2) with the prior (3.3), the joint posterior of all unknowns is:

$$\begin{aligned}\zeta\left(\phi_i's, \sigma^2, \boldsymbol{u}, \boldsymbol{\nu} \mid \boldsymbol{y}, \boldsymbol{H}\right) \quad \propto \quad & \zeta(\Theta|\boldsymbol{H}) \times \prod_{t=1}^{n}\left\{u_t^{1/2} p(u_t|\boldsymbol{\nu})\right\} \times (\sigma^2)^{-\frac{n}{2}} \times \\ & \exp\left\{-\frac{1}{2\sigma^2}\sum_{t=1}^{n} u_t\left(y_t - \boldsymbol{x}_t^T\boldsymbol{\beta}\right)^2\right\},\end{aligned} \tag{3.8}$$

This posterior is a nonlinear function of the DSAR coefficient vectors $\phi_i's$ through the cross-product terms in $\boldsymbol{\beta}$, and hence its marginals cannot be obtained analytically, underscoring the necessity of MCMC-based approximation. The full conditional distributions required for the MCMC-based approximation are derived in the next section.

4. Full conditionals and proposed algorithm for Bayesian inference of DSAR models

We now derive the full conditional posteriors for all model parameters and then combine them into a practical MCMC algorithm.

4.1. Full conditional posterior distributions

Conditional posterior of ϕ_i. To derive the conditional distribution of ϕ_i ($i = 1, 2, 3$) given all remaining parameters, we first restructure the matrix model (2.7) by isolating the dependence on ϕ_i:

$$\boldsymbol{y} \quad = \quad \boldsymbol{Z}_{\phi_i}\phi_i + \boldsymbol{L}_{\phi_i}\phi_{-i} + \boldsymbol{\varepsilon}, \tag{4.1}$$

Substituting this reparameterization into the joint posterior (3.8), completing the square in the exponent with respect to $\boldsymbol{\phi_i}$, and integrating out all unrelated terms yields a multivariate normal conditional: $\boldsymbol{\phi_i} \mid \cdot \sim N_{p_i}(\boldsymbol{\mu}^\star_{\boldsymbol{\phi_i}}, \boldsymbol{V}^\star_{\boldsymbol{\phi_i}})$. The posterior mean and covariance depend on the choice of prior and are given below.

For the normal-gamma prior:

$$
\begin{aligned}
\boldsymbol{\mu}^\star_{\boldsymbol{\phi_i}} &= \left[\left(\boldsymbol{Z}^T_{\phi_i}\boldsymbol{U}\boldsymbol{Z}_{\phi_i} + \boldsymbol{\Sigma}^{-1}_{\boldsymbol{\phi_i}}\right)^{-1}\left(\boldsymbol{Z}^T_{\phi_i}\boldsymbol{U}\left(\boldsymbol{y} - \boldsymbol{L}_{\phi_i}\boldsymbol{\phi_{-i}}\right) + \boldsymbol{\Sigma}^{-1}_{\boldsymbol{\phi_i}}\boldsymbol{\mu}_{\boldsymbol{\phi_i}}\right)\right], \text{ and} \\
\boldsymbol{V}^\star_{\boldsymbol{\phi_i}} &= \sigma^2\left(\boldsymbol{Z}^T_{\phi_i}\boldsymbol{U}\boldsymbol{Z}_{\phi_i} + \boldsymbol{\Sigma}^{-1}_{\boldsymbol{\phi_i}}\right)^{-1}.
\end{aligned}
\tag{4.2}
$$

For the g prior:

$$
\begin{aligned}
\boldsymbol{\mu}^\star_{\boldsymbol{\phi_i}} &= \left[\left(\boldsymbol{Z}^T_{\phi_i}\boldsymbol{G}\boldsymbol{Z}_{\phi_i}\right)^{-1}\left(g\boldsymbol{Z}^T_{\phi_i}(\boldsymbol{X}\bar{\boldsymbol{\beta}} - \boldsymbol{L}_{\phi_i}\boldsymbol{\phi_{-i}}) + \boldsymbol{Z}^T_{\phi_i}\boldsymbol{U}\left(\boldsymbol{y} - \boldsymbol{L}_{\phi_i}\boldsymbol{\phi_{-i}}\right)\right)\right], \text{ and} \\
\boldsymbol{V}^\star_{\boldsymbol{\phi_i}} &= \sigma^2\left(\boldsymbol{Z}^T_{\phi_i}\boldsymbol{G}\boldsymbol{Z}_{\phi_i}\right)^{-1}.
\end{aligned}
\tag{4.3}
$$

For Jeffreys' prior:

$$
\begin{aligned}
\boldsymbol{\mu}^\star_{\boldsymbol{\phi_i}} &= \left(\boldsymbol{Z}^T_{\phi_i}\boldsymbol{U}\boldsymbol{Z}_{\phi_i}\right)^{-1}\left(\boldsymbol{Z}^T_{\phi_i}\boldsymbol{U}\left(\boldsymbol{y} - \boldsymbol{L}_{\phi_i}\boldsymbol{\phi_{-i}}\right)\right), \text{ and} \\
\boldsymbol{V}^\star_{\boldsymbol{\phi_i}} &= \sigma^2\left(\boldsymbol{Z}^T_{\phi_i}\boldsymbol{U}\boldsymbol{Z}_{\phi_i}\right)^{-1}.
\end{aligned}
\tag{4.4}
$$

In the above expressions, $\boldsymbol{U} = \text{diag}(u_1, u_2, \ldots, u_n)$, $\boldsymbol{G} = \text{diag}(u_1 + g, u_2 + g, \ldots, u_n + g)$, and the matrices $\boldsymbol{Z}_{\phi_i}$ and $\boldsymbol{L}_{\phi_i}$ are constructed as detailed in Amin [2].

Conditional posterior of σ^2. Reading off the relevant terms in (3.8), the conditional posterior of the scale parameter is an inverse-gamma: $\sigma^2 \mid \cdot \sim IG(a/2, b/2)$, with hyperparameters determined by the prior choice.

Normal-gamma prior:

$$
\begin{aligned}
a &= a_0 + n + p_1 + p_2 + p_3, \\
b &= b_0 + \sum_{i=1}^{3}(\boldsymbol{\phi_i} - \boldsymbol{\mu}_{\boldsymbol{\phi_i}})^T\boldsymbol{\Sigma}^{-1}_{\boldsymbol{\phi_i}}(\boldsymbol{\phi_i} - \boldsymbol{\mu}_{\boldsymbol{\phi_i}}) + (\boldsymbol{y} - \boldsymbol{X}\boldsymbol{\beta})^T\boldsymbol{U}(\boldsymbol{y} - \boldsymbol{X}\boldsymbol{\beta}).
\end{aligned}
\tag{4.5}
$$

g prior:

$$
\begin{aligned}
a &= n + m, \\
b &= (\boldsymbol{\beta} - \bar{\boldsymbol{\beta}})^T(g\boldsymbol{X}^T\boldsymbol{X})(\boldsymbol{\beta} - \bar{\boldsymbol{\beta}}) + (\boldsymbol{y} - \boldsymbol{X}\boldsymbol{\beta})^T\boldsymbol{U}(\boldsymbol{y} - \boldsymbol{X}\boldsymbol{\beta}).
\end{aligned}
\tag{4.6}
$$

Jeffreys' prior:

$$
a = n \text{ and } b = (\boldsymbol{y} - \boldsymbol{X}\boldsymbol{\beta})^T\boldsymbol{U}(\boldsymbol{y} - \boldsymbol{X}\boldsymbol{\beta}). \tag{4.7}
$$

Conditional posteriors of $\boldsymbol{u}$ and $\boldsymbol{\nu}$. These quantities are SMN-case specific and are derived from the joint posterior (3.8) as follows.

SMN-t case. Each element u_t of $\boldsymbol{u}$ has a gamma conditional posterior with shape $(\nu+1)/2$ and rate $[(y_t - \boldsymbol{x}_t^T\boldsymbol{\beta})^2/(2\sigma^2) + \nu/2]$. The conditional posterior of the degrees-of-freedom parameter ν is:

$$\zeta\left(\nu \mid \boldsymbol{\phi}_i's, \sigma^2, \boldsymbol{u}, \boldsymbol{y}, \boldsymbol{H_1}, \lambda\right) \propto \left(\frac{(\nu/2)^{\nu/2}}{\Gamma(\nu/2)}\right)^n \exp\left\{-\nu\left(\frac{1}{2}\sum_{t=1}^n u_t + \lambda\right)\right\} \times \prod_{t=1}^n u_t^{\left(\frac{\nu}{2}-1\right)}, \quad \nu > 2. \tag{4.8}$$

This density is nonstandard, so we employ a Metropolis-Hastings step with a truncated normal proposal, restricted to $(2, \infty)$. The hyperparameter λ has a tractable conditional, which is a truncated gamma $TG(2, \nu, (c, d))$ with shape 2 and rate ν.

SMN-sl case. Each u_t follows a truncated gamma with shape $\nu + 1/2$ and rate $(y_t - \boldsymbol{x}_t^T\boldsymbol{\beta})^2/(2\sigma^2)$, truncated to $(0, 1)$. The conditional of ν is a truncated gamma $TG((n+1),\ \lambda - \sum_{t=1}^n \log u_t,\ (1, \infty))$, and λ again follows $TG(2, \nu, (c, d))$.

SMN-cn case. Each u_t is a two-point discrete variable: it equals γ with probability $\nu_1^*/(\nu_1^* + \nu_2^*)$ and 1 with probability $\nu_2^*/(\nu_1^* + \nu_2^*)$, where

$$\begin{aligned} \nu_1^* &= \nu\gamma^{1/2} \exp\left\{-\frac{\gamma}{2\sigma^2}\left(y_t - \boldsymbol{x}_t^T\boldsymbol{\beta}\right)^2\right\}, \\ \nu_2^* &= (1-\nu) \exp\left\{-\frac{1}{2\sigma^2}\left(y_t - \boldsymbol{x}_t^T\boldsymbol{\beta}\right)^2\right\}. \end{aligned} \tag{4.9}$$

The mixing proportion ν is conditionally beta with parameters $(\nu_0 + m_\gamma)$ and $(\nu_1 + n - m_\gamma)$, where

$$m_\gamma = \sum_{t=1}^n S_t, \quad \text{and} \quad S_t = \begin{cases} 1 & \text{if } u_t = \gamma \\ 0 & \text{if } u_t = 1 \end{cases}. \tag{4.10}$$

The conditional of γ is nonstandard:

$$\zeta\left(\gamma \mid \boldsymbol{\phi}_i's, \sigma^2, \boldsymbol{u}, \boldsymbol{y}, \boldsymbol{H_1}, \nu\right) \propto \gamma^{\gamma_0-1}(1-\gamma)^{\gamma_1-1} \times \prod_{t=1}^n \left\{\nu\gamma^{1/2} \exp\left\{-\frac{\gamma}{2\sigma^2}\left(y_t - \boldsymbol{x}_t^T\boldsymbol{\beta}\right)^2\right\} + (1-\nu)\exp\left\{-\frac{1}{2\sigma^2}\left(y_t - \boldsymbol{x}_t^T\boldsymbol{\beta}\right)^2\right\}\right\}. \tag{4.11}$$

Because this density is nonstandard, it is sampled using Metropolis-Hastings transitions employing a logit-normal proposal to ensure the parameter remains within $(0, 1)$.

4.2. Proposed MCMC algorithm for Bayesian inference of DSAR models

With all full conditional distributions established, we are now positioned to formulate the hybrid Gibbs–Metropolis-Hastings sampler described in Algorithm 1. The algorithm systematically cycles through the full conditionals derived in Section 4.1, resorting to Metropolis-Hastings transitions where the conditional is nonstandard.

Algorithm 1 Proposed MCMC algorithm for Bayesian inference of DSAR models

Inputs include: $\boldsymbol{y}$ time series dataset, s_1 and s_2 seasonal periods, and p_1, p_2, and p_3 orders of SAR model.
Apply the OLS method to estimate the $DSAR(p_1)(p_2)_{s_1}(p_3)_{s_2}$ model.
Set the priors for the DSAR parameters and set the OLS estimates as starting values for the MCMC simulations.
Set the MCMC simulations design:
  Number of simulations as $Nsim$.
  Burn-in as $Nburn$.
  Thinning level as $Nthin$.
for $r = 1 : Nsim$ **do** generate from the full conditional posterior distributions as:
  $\boldsymbol{\phi}_{\boldsymbol{i}}^{\boldsymbol{r}} \sim \zeta\left(\boldsymbol{\phi}_{\boldsymbol{i}}^{\boldsymbol{r}} \mid \boldsymbol{y}, \boldsymbol{u}^{\boldsymbol{r-1}}, \ \ldots\right) = N(\mu_{\phi_i}^{\star}, V_{\phi_i}^{\star}) \ \forall i,$
  $(\sigma^2)^r \sim \zeta\left((\sigma^2)^r \mid \boldsymbol{y}, \boldsymbol{u}^{\boldsymbol{r-1}}, \ \ldots\right) = IG(\frac{a}{2}, \frac{b}{2}),$
  Based on the SMN case:
  In the case of the SMN-t distribution:
  $u_t^r \sim \zeta\left(u_t^r \mid \boldsymbol{y}, \boldsymbol{\phi}_{\boldsymbol{i}}^{\boldsymbol{r}}, \ \ldots\right) = G\left(\frac{\nu+1}{2}, \left(\frac{(y_t - \boldsymbol{x}_t^T\boldsymbol{\beta})^2}{2\sigma^2} + \frac{\nu}{2}\right)\right) \ \forall t.$
  $\nu^r \sim \zeta\left(\nu^r \mid \boldsymbol{y}, \boldsymbol{u}^{\boldsymbol{r}}, \ \ldots\right)$ given in eqn. (4.8) with the Metropolis-Hastings.
  $\lambda^r \sim \zeta\left(\lambda^r \mid \boldsymbol{y}, \boldsymbol{u}^{\boldsymbol{r}}, \ \ldots\right) = TG(2, \nu, (c, d)).$
  In the case of the SMN-sl distribution:
  $u_t^r \sim \zeta\left(u_t^r \mid \boldsymbol{y}, \boldsymbol{\phi}_{\boldsymbol{i}}^{\boldsymbol{r}}, \ \ldots\right) = TG\left((\nu + \frac{1}{2}), \left(\frac{(y_t - \boldsymbol{x}_t^T\boldsymbol{\beta})^2}{2\sigma^2}\right), (0, 1)\right) \ \forall t.$
  $\nu^r \sim \zeta\left(\nu^r \mid \boldsymbol{y}, \boldsymbol{u}^{\boldsymbol{r}}, \ \ldots\right) = TG\left((n+1), \left(\lambda - \sum_{t=1}^{n} \log(u_t)\right), (1, \infty)\right).$
  $\lambda^r \sim \zeta\left(\lambda^r \mid \boldsymbol{y}, \boldsymbol{u}^{\boldsymbol{r}}, \ \ldots\right) = TG(2, \nu, (c, d)).$
  In the case of the SMN-cn distribution:
  $u_t^r \sim \zeta\left(u_t^r \mid \boldsymbol{y}, \boldsymbol{\phi}_{\boldsymbol{i}}^{\boldsymbol{r}}, \ \ldots\right) = \frac{\nu_1^*}{\nu_1^* + \nu_2^*} \mathbb{I}_{\{\gamma\}}(u_t) + \frac{\nu_2^*}{\nu_1^* + \nu_2^*} \mathbb{I}_{\{1\}}(u_t) \ \forall t.$
  $\nu^r \sim \zeta\left(\nu^r \mid \boldsymbol{y}, \boldsymbol{u}^{\boldsymbol{r}}, \ \ldots\right) = Beta\left((\nu_0 + m_\gamma), (\nu_1 + n - m_\gamma)\right).$
  $\gamma^r \sim \zeta\left(\gamma^r \mid \boldsymbol{y}, \boldsymbol{u}^{\boldsymbol{r}}, \ \ldots\right)$ given in eqn. (4.11) with the Metropolis-Hastings on the logit scale.
end for
In each loop, generated values represent together the r^{th} value of the MCMC chain, i.e., $\{\boldsymbol{\phi}_{\boldsymbol{1}}^{\boldsymbol{r}}, \boldsymbol{\phi}_{\boldsymbol{2}}^{\boldsymbol{r}}, \boldsymbol{\phi}_{\boldsymbol{3}}^{\boldsymbol{r}}, (\sigma^2)^r, \boldsymbol{u}^{\boldsymbol{r}}, \nu^r, \lambda^r, \gamma^r\}$.
Execute the burn-in and thinning by discarding the first $Nburn$ of the generated MCMC chain and selecting the $Nthin^{th}$ of the remaining chain.
Evaluate the convergence of generated MCMC chain using different convergence diagnostics.
Compute the posterior estimates of the DSAR parameters by averaging the convergent MCMC chain.

Prior to initiating the MCMC iterations, ordinary least squares (OLS) estimates serve a dual purpose: they provide starting values that accelerate convergence and offer a data-driven basis for eliciting weakly informative priors. Chain convergence is monitored throughout using the diagnostics of Geweke [31] and Raftery and Lewis [32], as well as inspection of within-chain autocorrelations; see also Amin [11] and LeSage [33] for implementation details. The burn-in and thinning procedures are employed to discard initial transient behavior and to reduce serial dependence in the retained draws, following standard recommendations in Robert and Casella [34] and Link and Eaton [35]. Posterior summaries—means, standard deviations, and credible intervals—are computed from the thinned post-burn-in portion of the chain.

Comparison with general-purpose MCMC software. Modern probabilistic programming languages such as Stan [36] and PyMC [37] implement Hamiltonian Monte Carlo (HMC) and no U-turn sampler (NUTS), which can reduce autocorrelation relative to standard Gibbs sampling. However, the custom Gibbs–Metropolis-Hastings sampler proposed here offers specific advantages in the DSAR–SMN setting. (i) The closed-form conjugate conditional updates for $\boldsymbol{\phi}_i$ and σ^2 exploit the analytical structure of the DSAR likelihood, avoiding the gradient evaluations required by HMC. (ii) The latent weights u_t are drawn exactly from n independent distributions in the Gibbs step, with zero autocorrelation, which HMC would handle less efficiently without custom marginalization. (iii) The sampler requires no external dependencies beyond standard distributions, facilitating reproducibility. Nonetheless, an empirical comparison of runtime, effective sample size per second, and parameter recovery against Stan or PyMC is a worthwhile direction for future work.

5. Simulation study and real applications

We assess the performance of the proposed MCMC algorithm through a controlled Monte Carlo study and illustrate its applicability on two electricity load datasets.

5.1. Simulation study

The simulation experiment is designed to span a variety of seasonal patterns and distributional scenarios. Four DSAR models are considered, each paired with a distinct SMN error distribution; the experimental configurations are summarized in Table 2.

Table 2. Setting of the simulation study.

Model	ϕ_{11}	ϕ_{12}	ϕ_{21}	ϕ_{22}	ϕ_{31}	σ^2	s_1	s_2	n	Distribution of Errors
I	0.6	-	0.4	-	0.3	1.0	5	25	1,000	SMN-cn ($\nu = 0.2, \gamma = 0.1$)
II	-0.4	-	0.5	-	0.7	1.0	5	25	1,000	SMN-sl ($\nu = 3$)
III	0.7	-0.4	0.3	-	0.5	1.0	5	25	1,000	SMN-t ($\nu = 10$)
IV	0.5	0.3	0.6	-0.4	0.3	1.0	24	168	2,000	SMN-t ($\nu = 5$)

For each model, 500 independent time series are generated, and the proposed MCMC algorithm is applied to every realization. Jeffreys' prior is adopted for $(\boldsymbol{\phi}_i's, \sigma^2)$, and case-specific priors are used for the SMN parameters as outlined in Section 3. The hyperparameters for the SMN-specific priors are fixed as follows. For the SMN-t and SMN-sl cases, the rate hyperparameter λ is assigned a Uniform(c, d) prior with $c = 0.01$ and $d = 0.5$, following Cabral et al. [30]. For the SMN-cn case, flat Beta priors are adopted with $\nu_0 = \nu_1 = \gamma_0 = \gamma_1 = 1$, corresponding to uniform priors on $(0, 1)$. These same hyperparameter choices are used in the real-data analysis in Section 5.2. The MCMC configuration is: total iterations $Nsim = 25{,}000$, burn-in $Nburn = 5{,}000$, thinning interval $Nthin = 20$, yielding 1,000 retained draws per run. Posterior summaries—mean, standard deviation, and 95% credible interval—are averaged across all 500 replications to obtain stable performance indicators. Estimation accuracy is further assessed via the coverage probability (CP)—the fraction of replications whose 95% credible interval contains the true value. A CP near 95% signals well-calibrated uncertainty.

Single realization results. Before presenting the aggregated results, we illustrate the algorithm behavior on a single realization from Model I (SMN-cn errors). Table 3 reports the Bayesian estimates, while Figure 1 presents the trace plots and marginal posterior densities for this representative dataset. Convergence diagnostics are also provided in Table 4.

Table 3. Simulation results for one time series dataset generated from Model I.

Parameter	Actual	$\mu^\star$	σ	L	U
ϕ_{11}	0.6	0.596	0.021	0.552	0.638
ϕ_{21}	0.4	0.393	0.021	0.351	0.434
ϕ_{31}	0.3	0.281	0.023	0.236	0.325
σ^2	1.0	0.986	0.243	0.814	1.747
ν	0.2	0.190	0.044	0.131	0.300
γ	0.1	0.087	0.100	0.061	0.420

$\star$ μ and σ: Posterior mean and standard deviation.
L and U: Limits of the 95% credible interval.

Table 4. Convergence diagnostics of DSAR parameters for one time series generated from Model I.

	Raftery–Lewis diagnostic			Geweke Z-statistic		Autocorrelations		
Param	*Ntotal*	*Nmin*	*Factor*	z-score	p-value	Lag 5	Lag 10	Lag 50
ϕ_{11}	893	937	0.953	0.665	0.506	0.006	0.091	0.019
ϕ_{21}	893	937	0.953	-1.274	0.203	0.059	0.038	-0.039
ϕ_{31}	1053	937	1.124	-1.104	0.270	0.045	0.020	0.047
σ^2	893	937	0.953	0.666	0.505	0.016	0.018	-0.050
ν	969	937	1.034	-1.167	0.243	0.001	0.028	-0.045
γ	1053	937	1.124	0.799	0.424	-0.042	0.064	-0.011

The single-replication results confirm that the posterior means closely track the true parameter values with small dispersion, and the 95% credible intervals consistently include the true parameter values. Chain convergence is evaluated using the Geweke z-test [31], the Raftery–Lewis diagnostic [32], and sample autocorrelations, as reported in Table 3. For the representative replication of Model I, all Geweke z-scores for the DSAR parameters lie within $(-2, 2)$, and the Raftery–Lewis diagnostic [32] indicates that fewer than 1,000 iterations are sufficient across all parameters. The within-chain autocorrelations of the thinned draws are negligible across all lags, indicating that the thinning interval $N_{\text{thin}} = 20$ is sufficient to produce approximately independent posterior samples. This conclusion is further supported by the trace plots in Figure 1. The MCMC settings ($N_{\text{sim}} = 25{,}000$, $N_{\text{burn}} = 5{,}000$, $N_{\text{thin}} = 20$, yielding 1,000 retained draws) are chosen based on these diagnostics to ensure adequate burn-in removal and effective sample sizes for all parameters.

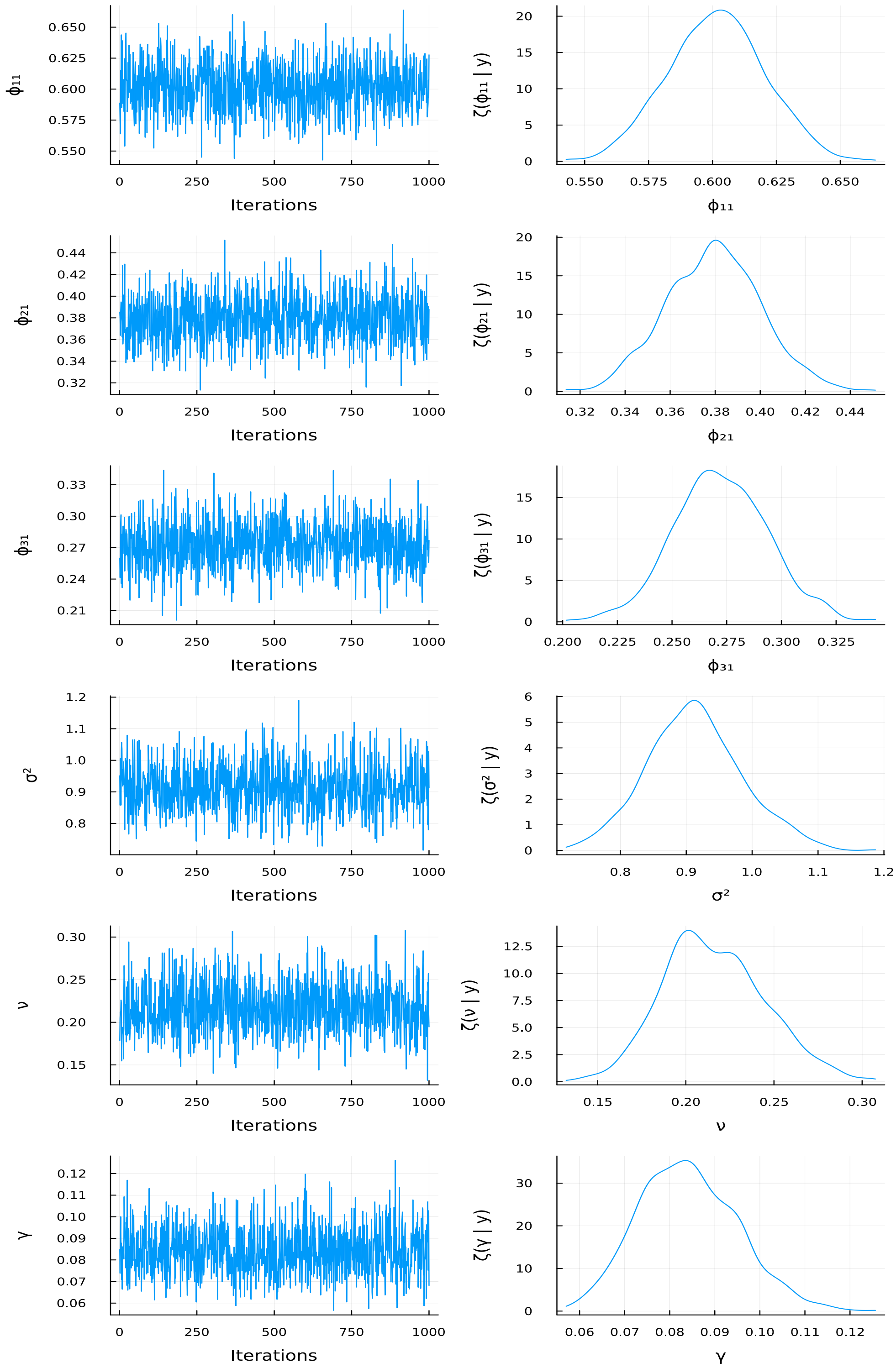

Figure 1. Trace plots and posteriors of DSAR parameters for one time series generated from Model I.

Aggregated Bayesian results. Table 5 presents the aggregated Bayesian results for Models I through IV, each estimated under Jeffreys' prior.

Table 5. Simulation results for Models I–IV estimated under Jeffreys' prior.

Param	Actual	μ	σ	L	U	$CP(\%)^{\star}$	Actual	μ	σ	L	U	$CP(\%)$
	Model I						Model II					
ϕ_{11}	0.6	0.600	0.020	0.561	0.638	95.6	-0.4	-0.400	0.029	-0.456	-0.342	95.2
ϕ_{21}	0.4	0.398	0.022	0.356	0.443	94.0	0.5	0.496	0.028	0.443	0.551	92.6
ϕ_{31}	0.3	0.298	0.023	0.255	0.343	94.8	0.7	0.699	0.023	0.654	0.743	95.2
σ^2	1.0	0.999	0.086	0.840	1.174	95.6	1.0	1.001	0.096	0.826	1.202	97.2
ν	0.2	0.209	0.033	0.151	0.284	96.2	3.0	2.973	0.716	2.084	4.832	97.8
γ	0.1	0.103	0.014	0.077	0.133	94.2	—	—	—	—	—	—
	Model III						Model IV					
ϕ_{11}	0.7	0.698	0.029	0.642	0.754	95.4	0.5	0.498	0.020	0.459	0.537	93.0
ϕ_{12}	-0.4	-0.404	0.029	-0.460	-0.349	96.4	0.3	0.299	0.020	0.259	0.338	96.0
ϕ_{21}	0.3	0.298	0.030	0.238	0.358	93.2	0.6	0.599	0.020	0.560	0.635	94.5
ϕ_{22}	—	—	—	—	—	—	-0.4	-0.399	0.019	-0.436	-0.362	95.0
ϕ_{31}	0.5	0.498	0.027	0.444	0.550	96.0	0.3	0.296	0.020	0.257	0.336	96.5
σ^2	1.0	0.995	0.073	0.860	1.148	95.0	1.0	0.975	0.056	0.872	1.090	93.0
ν	10.0	10.104	3.771	6.230	20.707	94.2	5.0	4.807	0.564	3.890	6.098	94.0

$^{\star}CP(\%)$: Empirical coverage probability.

Across all four models and all three SMN distributional scenarios, the posterior means align closely with the prescribed true values, and the average 95% credible intervals contain the truth in every case. As shown in Table 5, the empirical coverage probabilities remain near the nominal 95% benchmark, ranging from roughly 93% to 98%. This alignment with the target level demonstrates that the posterior uncertainty quantification is appropriately calibrated, with credible intervals that avoid both systematic undercoverage and undue conservatism.

The SMN-t degrees-of-freedom parameter ν displays higher posterior variability relative to its mean than the structural parameters, reflecting the well-known identification challenges associated with moderate values of ν [22]. Despite this, the 95% credible intervals consistently cover the true values, and the empirical coverage probabilities remain close to nominal. Analogous patterns of accurate recovery are observed for the SMN-sl shape parameter ν and for the contamination parameters (ν, γ) in the SMN-cn model.

Prior sensitivity. To assess sensitivity to prior choice, Model I (SMN-cn) is additionally estimated under the normal-gamma and Zellner's g priors. For the normal-gamma prior, the precision matrix $\boldsymbol{\Sigma}_{\boldsymbol{\phi}_i}^{-1}$ controls how tightly the coefficients are shrunk toward the prior mean $\boldsymbol{\mu}_{\boldsymbol{\phi}_i}$. Two settings are considered:

1. *Weakly informative:* $\boldsymbol{\mu}_{\boldsymbol{\phi}_i} = \mathbf{0}$, $\boldsymbol{\Sigma}_{\boldsymbol{\phi}_i}^{-1} = 0.01\,\boldsymbol{I}$, $(a_0,\, b_0) = (0.01,\, 0.01)$; and
2. *Moderately informative:* $\boldsymbol{\mu}_{\boldsymbol{\phi}_i} = \mathbf{0}$, $\boldsymbol{\Sigma}_{\boldsymbol{\phi}_i}^{-1} = 1.0\,\boldsymbol{I}$, $(a_0,\, b_0) = (0.1,\, 0.1)$.

For Zellner's g prior, the scalar g rescales the reference covariance $(\boldsymbol{X}^T\boldsymbol{X})^{-1}$; two values are examined: $g = n^{-1}$ (unit-information prior) and $g = m^{-2}$, where $m = (1+p_1)(1+p_2)(1+p_3)-1$ denotes the number of regressors. Table 6 presents the Bayesian results for Model I estimated under the normal-gamma and g priors with these different settings.

Table 6. Simulation results for Model I estimated under normal-gamma and g priors with different settings.

Param	Actual	μ	σ	L	U	$CP(\%)$	μ	σ	L	U	$CP(\%)$
		Normal-gamma prior									
		$\Sigma_{\phi_i}^{-1} = 0.01\boldsymbol{I}$ and $(a_0, b_0) = (0.01, 0.01)$					$\Sigma_{\phi_i}^{-1} = 1.0\boldsymbol{I}$ and $(a_0, b_0) = (0.1, 0.1)$				
ϕ_{11}	0.6	0.6000	0.0195	0.5613	0.6378	95.8	0.5998	0.0195	0.5619	0.6377	95.8
ϕ_{21}	0.4	0.3981	0.0224	0.3559	0.4423	93.6	0.3980	0.0224	0.3558	0.4422	93.6
ϕ_{31}	0.3	0.2980	0.0225	0.2559	0.3426	94.6	0.2979	0.0225	0.2552	0.3421	95.0
σ^2	1.0	0.9712	0.0851	0.8137	1.1452	93.2	0.9743	0.0851	0.8171	1.1468	94.0
ν	0.2	0.2147	0.0342	0.1560	0.2928	94.2	0.2140	0.0342	0.1557	0.2911	94.2
γ	0.1	0.1022	0.0140	0.0770	0.1321	93.4	0.1022	0.0141	0.0768	0.1323	93.2
		Zellner's g prior									
		$g = n^{-1}$					$g = m^{-2}$				
ϕ_{11}	0.6	0.6000	0.0195	0.5617	0.6377	96.0	0.6001	0.0192	0.5622	0.6370	95.6
ϕ_{21}	0.4	0.3981	0.0223	0.3563	0.4425	93.6	0.3982	0.0220	0.3564	0.4419	93.6
ϕ_{31}	0.3	0.2978	0.0224	0.2560	0.3427	95.0	0.2978	0.0221	0.2558	0.3416	95.0
σ^2	1.0	0.9712	0.0852	0.8139	1.1456	93.2	0.9730	0.0852	0.8151	1.1461	93.2
ν	0.2	0.2143	0.0342	0.1555	0.2927	94.2	0.2143	0.0342	0.1557	0.2918	94.4
γ	0.1	0.1021	0.0140	0.0769	0.1317	93.4	0.1021	0.0140	0.0768	0.1320	93.6

The results in Table 6 reveal a high degree of stability across all prior specifications, which is also consistent with the Jeffreys' prior results reported in Table 5. We summarize the key findings below.

AR coefficients. The posterior means for ϕ_{11}, ϕ_{21}, and ϕ_{31} are essentially identical across all four prior settings, differing from the Jeffreys' estimates ($\hat{\mu}$ = 0.599, 0.398, 0.298) by at most 0.002 in absolute value—well within one posterior standard deviation in each case. Posterior standard deviations ($\approx$ 0.019–0.023) are likewise stable and match those under Jeffreys' prior to three decimal places. CPs are close to the nominal 95% level for all settings, ranging from 93.6% to 96.0%, compared to 94.0%–95.6% under Jeffreys' prior.

Variance parameter σ^2. The most discernible—yet still modest—difference relative to Jeffreys' prior concerns σ^2. Under Jeffreys' prior, the posterior mean is $\hat{\mu} = 0.999$, very close to the true value, with CP = 95.6% at the nominal level. Under the alternative priors, posterior means range from 0.971 to 0.974, representing a downward shift of roughly 0.025–0.028, with CPs in the range 93.2%–94.0%. This mild underestimation is attributable to the mild regularization imposed on $\boldsymbol{\beta}$: shrinking the coefficients toward zero slightly understates the residual variation, which propagates to the posterior of σ^2. The effect is consistent in direction across both normal-gamma settings and both g-prior values, but small in magnitude (less than 3% of the true value), and does not impair the practical utility of the estimates. Jeffreys' non-informative prior on σ^2 (corresponding formally to $a_0 = b_0 = 0$) avoids this interaction and achieves the coverage closest to 95%.

SMN-cn parameters ν and γ. The contamination-proportion parameter ν and the contamination-scale parameter γ are remarkably stable across all prior settings. The posterior mean of ν ranges from 0.2140 to 0.2147 under the alternative priors, compared to 0.209 under Jeffreys' prior. For γ, the posterior means (0.1021–0.1022) are virtually indistinguishable from the Jeffreys' estimate (0.103), and posterior standard deviations agree to four decimal places ($\hat{\sigma} = 0.014$ in all cases).

Within-family comparisons. Within the normal-gamma family, the weakly and moderately informative settings produce nearly identical posteriors (maximum difference in posterior means < 0.003; maximum difference in CPs ≤ 0.8 percentage points), indicating that doubling the prior precision from $0.01\boldsymbol{I}$ to $\boldsymbol{I}$—a hundredfold increase in regularization strength—has negligible impact on inference at this sample size. Within the g-prior family, the two scaling choices ($g = n^{-1}$ and $g = m^{-2}$) likewise produce nearly identical results for σ^2, ν, and γ, with only the marginally tighter AR posteriors under $g = m^{-2}$.

Metropolis-Hastings acceptance rates and MCMC convergence. For the SMN-t specification, the degrees-of-freedom parameter ν exhibits an average acceptance rate of Metropolis-Hastings of approximately 95%. This exceptionally high rate is a direct consequence of the tailored proposal density, which evaluates dynamic first- and second-order numerical derivatives via automatic differentiation to accurately approximate the conditional posterior distribution at each MCMC sweep. Consequently, this structural choice eliminates typical random walk behavior and minimizes chain autocorrelation. Conversely, for the SMN-cn specification, the mixing weight parameter γ is updated via a classical random walk Metropolis-Hastings step on the logit scale. The empirical acceptance rate settles at approximately 43%, aligning perfectly with the theoretically established optimal target for univariate random walk samplers [38]. Across simulation Models I–IV, the MCMC chains satisfy all convergence diagnostics, ensuring that the reported Bayesian estimates of the DSAR models are derived from properly converged chains.

Overall assessment. Collectively, these results confirm that the Bayesian inference of DSAR models under SMN errors is robust to the choice of prior specification. All alternative settings recover the true parameter values with small bias and CPs near 95%. Jeffreys' prior remains the recommended default for the DSAR–SMN framework, as it avoids the parameter coupling noted above and consistently achieves the best coverage for σ^2. These results provide compelling evidence that the proposed MCMC algorithm reliably recovers the DSAR parameters under a broad range of heavy-tailed error structures.

5.2. *Real applications on hourly electricity load*

To further validate the practical utility of the proposed methodology, we model hourly electricity consumption data from Croatia and Italy, both of which are well-known to exhibit a doubly seasonal structure—an intraday cycle of period 24 and a weekly cycle of period 168 [39]. The data comprises eight consecutive weeks of hourly readings beginning on Monday, 29 January 2024, and are plotted in Figures 2 and 3. The data was retrieved from the ENTSO-E Transparency Platform, a publicly accessible repository of European electricity system data, available at `https://transparency.entsoe.eu`.

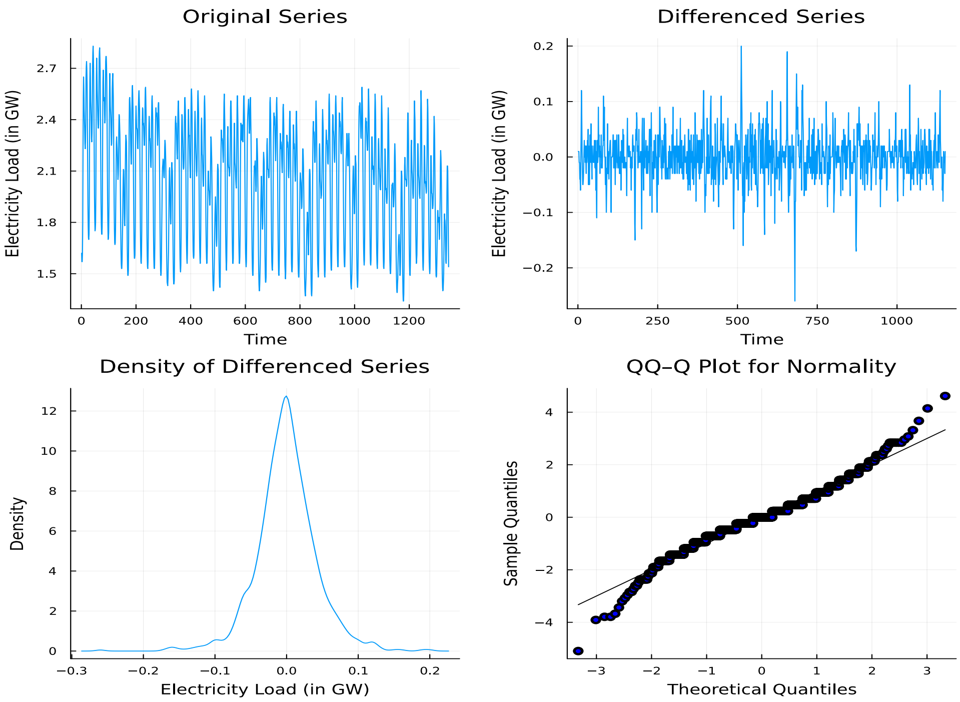

Figure 2. Time series, differenced series, empirical density, and Q-Q plots of hourly electricity load in Croatia.

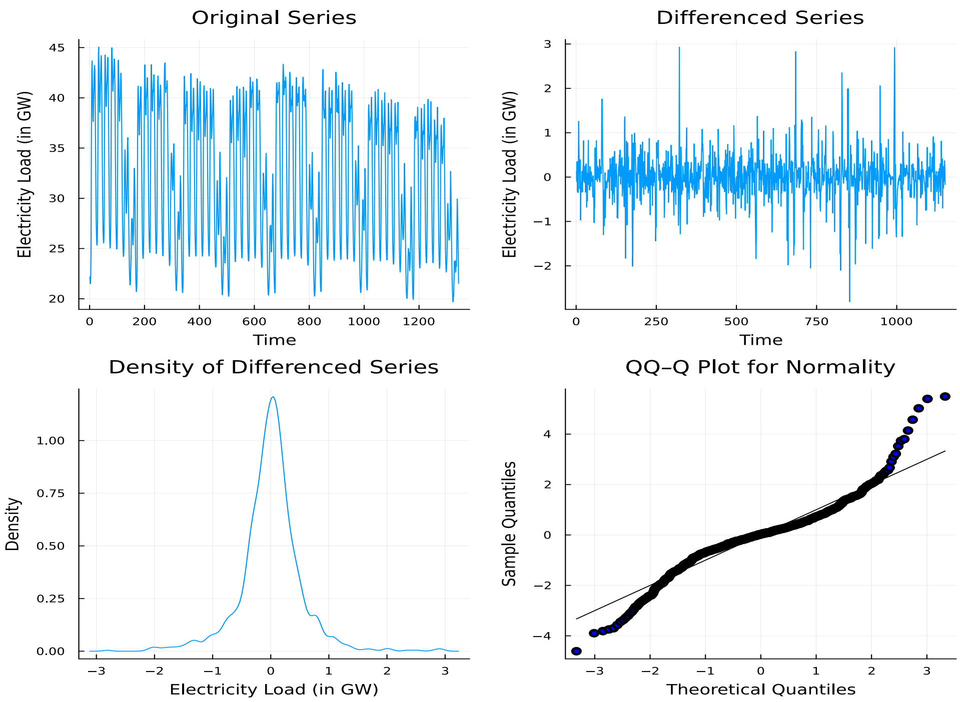

Figure 3. Time series, differenced series, empirical density, and Q-Q plots of hourly electricity load in Italy.

Figures 2 and 3 reveal clear nonstationarity in the raw series for both countries. Applying combined nonseasonal and seasonal differencing removes this trend and yields the stationary series shown in the figures. In addition, the empirical density plots in Figures 2 and 3 exhibit pronounced departure from normality, with elongated heavy tails, motivating the SMN error assumption. To further verify the heavy-tailed assumption, we present in Figures 2 and 3 the quantile–quantile (Q–Q) plots of these series against the normal distribution that reveal clear departures from the reference line in both tails. In addition, we apply the Shapiro–Wilk test that rejects normality at the 1% level for both countries.

The Bayesian information criterion (BIC) [40] is used to select the DSAR order for each stationary series. Candidate models of orders $p_1, p_2, p_3 \in \{0, 1, \cdots, 4\}$ are fitted by OLS on the stationary series, and the model with the smallest BIC is retained. The BIC-selected orders are DSAR$(1)(1)_{24}(3)_{168}$ for Croatia's series and DSAR$(1)(2)_{24}(3)_{168}$ for Italy's series. Whilst this order-selection step is not fully Bayesian, the subsequent MCMC analysis provides full posterior uncertainty quantification for all DSAR parameters of the selected model, which is the primary inferential goal of the paper. Both models are estimated via the proposed algorithm using the four SMN specifications of errors under Jeffreys' prior, with the same MCMC settings as in the simulation study.

To formally compare the competing error specifications, we compute the deviance information criterion (DIC) [41] for the estimated DSAR models under different SMN specifications for both countries, and the DIC values are reported in Table 7. For Croatia's series, the SMN-*t* specification achieves the lowest DIC, whereas for Italy's series the SMN-*cn* model provides the best fit. In both cases, these heavy-tailed alternatives yield substantially smaller DIC values than the Gaussian benchmark. Tables 8 and 9 summarize the posterior results of the best-fitting models relative to the Gaussian benchmark for both countries, while Figures 4 and 5 display the marginal posterior densities of the estimated coefficients.

All estimated DSAR coefficients are statistically relevant, as evidenced by their 95% credible intervals excluding zero. Notably, the SMN-*t* and SMN-cn models yield a substantially lower posterior estimate of σ^2 relative to the Gaussian specification for both countries, consistent with the well-documented bias inflation in scale estimation when heavy-tailed data is analyzed under incorrect Gaussian assumptions [22, 42]. In particular, the estimated degrees-of-freedom parameter $\hat{\nu} \approx 8.5$ for Croatia's series signals pronounced heavy-tailedness in the residuals. For Italy's series, the SMN-cn estimates $\hat{\nu} \approx 0.41$ and $\hat{\gamma} \approx 0.09$ imply that approximately 41% of observations arise from a contaminating component whose variance is inflated by a factor of $1/\hat{\gamma} \approx 11$ relative to the nominal component. These parameter estimates provide compelling evidence that the SMN-*t* and SMN-cn specifications capture distributional features of the electricity load residuals that are entirely masked by the normal model. The convergence of both MCMC chains is monitored and confirmed using various diagnostics, which are presented for the case of Italy's series in Table 10. These findings collectively validate the accuracy and practical relevance of the proposed MCMC framework for doubly seasonal time series.

Table 7. DIC for the estimated DSAR models under SMN errors for electricity load in Croatia and Italy.

	Croatia			Italy		
Model	$\bar{D}$	p_D	DIC	$\bar{D}$	p_D	DIC
SMN-*t*	-2878.31	6.82	-2871.49	334.98	7.62	342.60
SMN-*cn*	-2877.54	7.32	-2870.22	315.98	9.16	325.14
SMN-*sl*	-2876.87	6.76	-2870.11	349.50	7.13	356.63
SMN-*n* (Gaussian)	-2866.07	5.94	-2860.13	456.79	7.06	463.85

Table 8. Bayesian estimates of DSAR models for electricity load in Croatia.

	MCMC with SMN-*t* Errors				MCMC with SMN-n Errors			
Param	μ	σ	L	U	μ	σ	L	U
ϕ_{11}	0.3102	0.0403	0.2309	0.3855	0.3257	0.0394	0.2436	0.4039
ϕ_{21}	-0.4998	0.0326	-0.5607	-0.4326	-0.4953	0.0330	-0.5603	-0.4327
ϕ_{31}	-0.7671	0.0365	-0.8362	-0.6922	-0.7979	0.0339	-0.8598	-0.7297
ϕ_{32}	-0.5563	0.0411	-0.6461	-0.4782	-0.5826	0.0411	-0.6588	-0.5009
ϕ_{33}	-0.2790	0.0365	-0.3537	-0.2115	-0.3092	0.0362	-0.3813	-0.2349
$\sigma^2 \times 10^{-3}$	0.4479	0.0420	0.3713	0.5316	0.5826	0.0339	0.5230	0.6563
ν	8.4598	3.2627	4.9263	17.510	—	—	—	—

Table 9. Bayesian estimates of DSAR models for electricity load in Italy.

	MCMC with SMN-cn Errors				MCMC with SMN-n Errors			
Param	μ	σ	L	U	μ	σ	L	U
ϕ_{11}	0.2425	0.0312	0.1812	0.3018	0.2567	0.0387	0.1820	0.3336
ϕ_{21}	-0.7165	0.0335	-0.7864	-0.6538	-0.7071	0.0393	-0.7814	-0.6302
ϕ_{22}	-0.3247	0.0326	-0.3861	-0.2578	-0.3647	0.0389	-0.4367	-0.2857
ϕ_{31}	-0.6977	0.0340	-0.7628	-0.6320	-0.7426	0.0397	-0.8159	-0.6616
ϕ_{32}	-0.4962	0.0390	-0.5759	-0.4265	-0.5797	0.0472	-0.6705	-0.4838
ϕ_{33}	-0.2174	0.0306	-0.2775	-0.1585	-0.2522	0.0429	-0.3295	-0.1660
σ^2	0.0237	0.0036	0.0175	0.0315	0.1255	0.0074	0.1126	0.1404
ν	0.4068	0.0473	0.3117	0.4952	—	—	—	—
γ	0.0847	0.0132	0.0618	0.1143	—	—	—	—

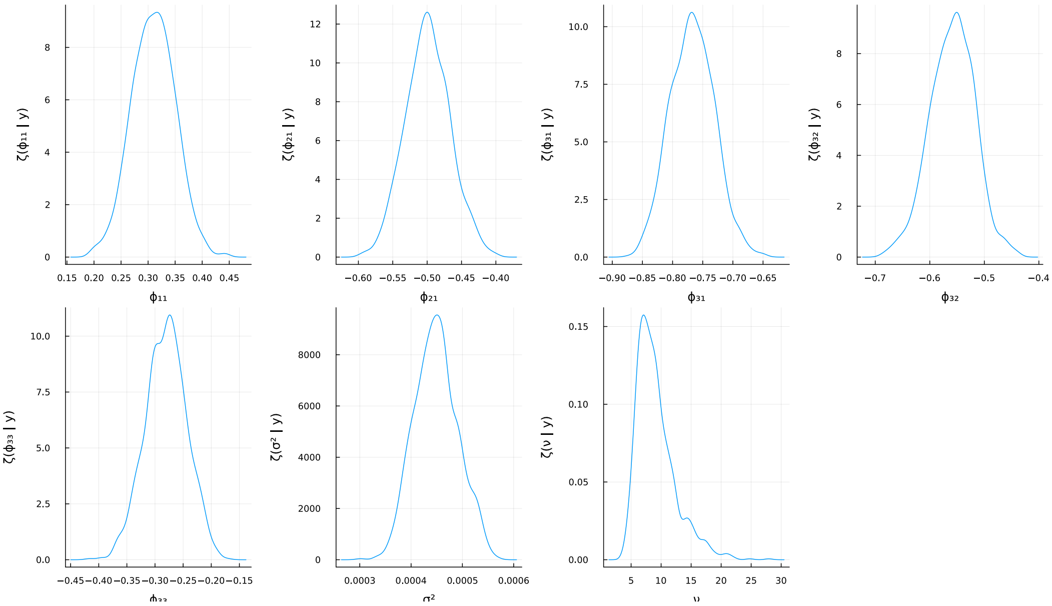

Figure 4. Posteriors of the DSAR model with SMN-*t* for the electricity load in Croatia.

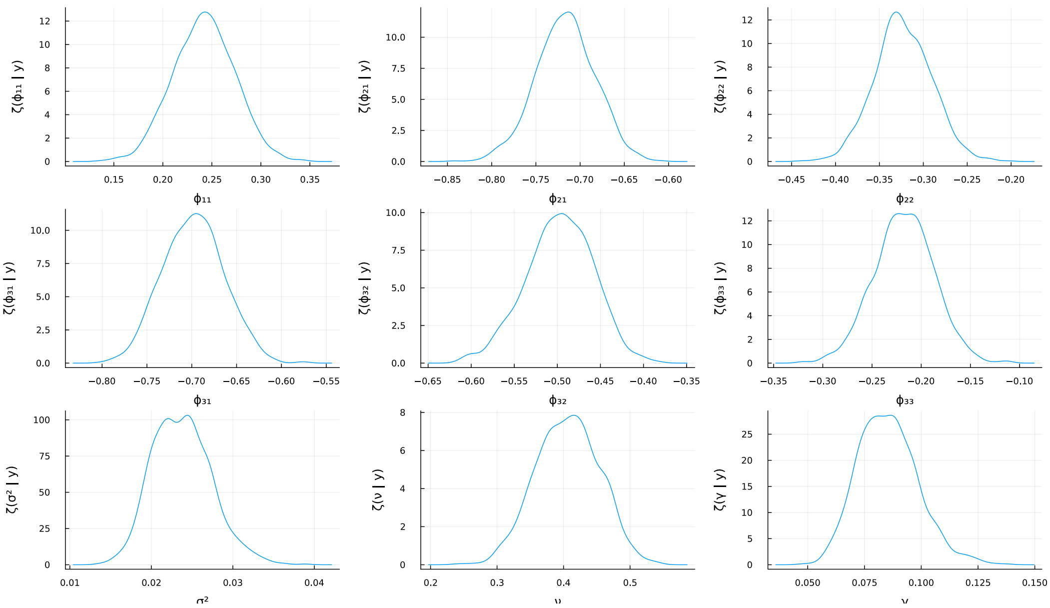

Figure 5. Posteriors of the DSAR model with SMN-cn for the electricity load in Italy.

Table 10. Convergence diagnostics of DSAR parameters for the electricity load in Italy.

	Raftery–Lewis diagnostic			Geweke Z-statistic		Autocorrelations		
Param	*Ntotal*	*Nmin*	*Factor*	z-score	p-value	Lag 5	Lag 10	Lag 50
ϕ_{11}	969	937	1.034	1.173	0.241	0.017	-0.002	-0.025
ϕ_{21}	969	937	1.034	-0.218	0.828	-0.021	0.018	-0.024
ϕ_{22}	969	937	1.034	1.369	0.171	-0.059	-0.040	-0.055
ϕ_{31}	893	937	0.953	-0.377	0.706	0.028	-0.014	-0.037
ϕ_{32}	893	937	0.953	1.331	0.183	-0.008	-0.035	-0.027
ϕ_{33}	1053	937	1.124	-0.419	0.675	-0.023	0.003	-0.042
σ^2	1143	937	1.220	0.193	0.847	0.030	-0.040	-0.063
ν	1053	937	1.124	-0.341	0.733	0.028	0.018	-0.025
γ	1053	937	1.124	0.323	0.747	-0.010	-0.009	-0.031

6. Conclusions

This paper presented a comprehensive Bayesian inferential framework for multiplicative DSAR models under the SMN distributional assumption for the error terms. By treating the latent scale factors as auxiliary variables, we derived closed-form full conditional posteriors for the DSAR coefficient vectors and the scale parameter, i.e., multivariate normal and inverse-gamma distributions, under three prior specifications: normal-gamma, g, and Jeffreys. The conditional posteriors of the SMN-specific parameters were also obtained in closed form, though certain members require Metropolis-Hastings transitions because they do not correspond to standard distributional families. Combining these results, we constructed a hybrid Gibbs–Metropolis-Hastings algorithm that provides efficient and principled posterior approximation for the entire parameter set. Extensive Monte Carlo experiments across four DSAR configurations encompassing three distinct SMN error distributions confirmed the accuracy of the proposed sampler. Real-data analyses of hourly electricity load in Croatia and Italy demonstrated the practical relevance of the MCMC framework. Future work may include a systematic comparison of the proposed MCMC sampler with Hamiltonian Monte Carlo implementations available in platforms such as Stan and PyMC.

Author contributions

Ayman A. Amin: Writing—original draft, methodology, software, validation; Farouq Mohammad A. Alam: Writing—review & editing, project administration, funding acquisition. All authors have read and approved the final version of the manuscript for publication.

Use of Generative-AI tools declaration

The authors declare they have not used Artificial Intelligence (AI) tools in the creation of this article.

Acknowledgments

The authors are thankful to the Deanship of Graduate Studies and Scientific Research at Najran University for funding this work under the Consortium Funding Program grant code (NU/CPL/SERC/14/4440-4). Moreover, the authors sincerely thank the handling editor and the anonymous reviewers for their constructive feedback, which significantly enhanced the clarity and quality of this manuscript.

The project was funded by the KAU Endowment (WAQF) at King Abdulaziz University, Jeddah, Saudi Arabia. The authors, therefore, gratefully acknowledge WAQF and the Deanship of Scientific Research (DSR) for technical and financial support.

Conflict of interest

The authors declare no conflicts of interest.

References

1. A. A. Amin, W. Emam, Y. Tashkandy, C. Chesneau, Bayesian subset selection of seasonal autoregressive models, *Math.*, **11** (2023), 1–13. https://doi.org/10.3390/math11132878

2. A. A. Amin, Full bayesian analysis of double seasonal autoregressive models with real applications, *J. Appl. Stat.*, **51** (2024), 1524–1544. https://doi.org/10.1080/02664763.2023.2211754

3. S. Shaarawy, M. Ismail, Bayesian inference for seasonal arma models, *Egypt. Stat. J.*, **31** (1987), 323–336. https://doi.org/10.21608/esju.1987.428903

4. A. A. Amin, S. A. Alghamdi, Bayesian identification procedure for triple seasonal autoregressive models, *Mathematics*, **11** (2023), 3823. https://doi.org/10.3390/math11183823

5. G. Barnett, R. Kohn, S. Sheather, Bayesian estimation of an autoregressive model using markov chain monte carlo, *J. Econom.*, **74** (1996), 237–254. https://doi.org/10.1016/0304-4076(95)01744-5

6. G. Barnett, R. Kohn, S. Sheather, Robust bayesian estimation of autoregressive–moving-average models, *J. Time Ser. Anal.*, **18** (1997), 11–28. https://doi.org/10.1111/1467-9892.00036

7. J. Vermaak, M. Niranjan, S. J. Godsill, *Markov chain Monte Carlo estimation for the seasonal autoregressive process with application to pitch modelling*, Technical report, Department of Engineering, University of Cambridge, 1998.

8. M. A. Ismail, A. A. Amin, Gibbs sampling for sarma models, *Pak. J. Stat.*, **30** (2014), 153–168.

9. A. A. Amin, Gibbs sampling for bayesian prediction of sarma processes, *Pak. J. Stat. Oper. Res.*, **15** (2019), 397–418. https://doi.org/10.18187/pjsor.v15i2.2174

10. A. A. Amin, M. A. Ismail, Gibbs sampling for double seasonal autoregressive models, *Commun. Stat. Appl. Method.*, **22** (2015), 557–573. https://doi.org/10.5351/CSAM.2015.22.6.557

11. A. A. Amin, Bayesian analysis of double seasonal autoregressive models, *Sankhya B*, **82** (2020), 328–352. https://doi.org/10.1007/s13571-019-00192-z

12. G. Ferreira, L. M. Castro, V. H. Lachos, R. Dias, Bayesian modeling of autoregressive partial linear models with scale mixture of normal errors, *J. Appl. Stat.*, **40** (2013), 1796–1816. https://doi.org/10.1080/02664763.2013.796349

13. M. R. Mahmoudi, M. Maleki, D. Baleanu, V. T. Nguyen, K. H. Pho, A bayesian approach to heavy-tailed finite mixture autoregressive models, *Symmetry*, **12** (2020), 929. https://doi.org/10.3390/sym12060929

14. H. Ryu, D. H. Kim, Robust bayesian analysis for autoregressive models, *J. Korean Data Inf. Sci. Soc.*, **26** (2015), 487–493. https://doi.org/10.7465/jkdi.2015.26.2.487

15. M. Agarwal, P. K. Tripathi, Classical and bayes analyses of autoregressive model with heavy-tailed error, *Am. J. Math. Manag. Sci.*, **43** (2024), 40–60. https://doi.org/10.1080/01966324.2024.2309387

16. A. A. Amin, S. A. Alghamdi, Bayesian estimation of autoregressive models with exogenous variables under scale-mixtures of normal errors, *Mathematics*, **14** (2026), 2188. https://doi.org/10.3390/math14122188

17. A. A. Amin, Bayesian modeling and forecasting of seasonal autoregressive models with scale-mixtures of normal errors, *Comput. Stat.*, **40** (2025), 3453–3475. https://doi.org/10.1007/s00180-025-01617-2

18. A. A. Amin, Full bayesian analysis of seasonal autoregressive models under scale-mixtures of normal errors, *J. Stat. Comput. Simul.*, **96** (2026), 184–204. https://doi.org/10.1080/00949655.2025.2556269

19. D. F. Andrews, C. L. Mallows, Scale mixtures of normal distributions, *J. R. Stat. Soc. Ser. B*, **36** (1974), 99–102. https://doi.org/10.1111/j.2517-6161.1974.tb00989.x

20. M. West, On scale mixtures of normal distributions, *Biometrika*, **74** (1987), 646–648.

21. M. A. Tanner, W. H. Wong, The calculation of posterior distributions by data augmentation, *J. Am. Stat. Assoc.*, **82** (1987), 528–540. https://doi.org/10.2307/2289457

22. K. L. Lange, R. J. A. Little, J. M. G. Taylor, Robust statistical modeling using the t distribution, *J. Am. Stat. Assoc.*, **84** (1989), 881–896. https://doi.org/10.1080/01621459.1989.10478852

23. W. H. Rogers, J. W. Tukey, Understanding some long-tailed symmetrical distributions, *Stat. Neerl.*, **26** (1972), 211–226. https://doi.org/10.1111/j.1467-9574.1972.tb00191.x

24. J. W. Tukey, A survey of sampling from contaminated distributions, in *Contrib. Probab. Stat.* (ed. I. Olkin). Stanford Univ. Press, Stanford, CA, 1960, 448–485.

25. A. Gelman, J. B. Carlin, H. S. Stern, D. B. Rubin, *Bayesian Data Analysis*, 2nd edition, Chapman & Hall/CRC, Boca Raton, FL, 2004, https://doi.org/10.1201/9780429258480

26. A. Zellner, On assessing prior distributions and Bayesian regression analysis with g-prior distributions, in *Bayesian Inference Decision Tech.: Essays Honor Bruno de Finetti* (eds. P. Goel and A. Zellner). North-Holland/Elsevier, Amsterdam, 1986, 233–243.

27. C. Fernandez, E. Ley, M. F. Steel, Benchmark priors for bayesian model averaging, *J. Econom.*, **100** (2001), 381–427. https://doi.org/10.1016/S0304-4076(00)00076-2

28. A. A. Amin, Kullback-leibler divergence to evaluate posterior sensitivity to different priors for autoregressive time series models, *Commun. Stat. Simul. Comput.*, **48** (2019), 1277–1291. https://doi.org/10.1080/03610918.2017.1410709

29. H. Jeffreys, *Theory of Probability*, 3rd edition, Oxford Univ. Press, Oxford, 1961.

30. C. R. B. Cabral, V. H. Lachos, M. R. Madruga, Bayesian analysis of skew-normal independent linear mixed models with heterogeneity in the random-effects population, *J. Stat. Plann. Inference*, **142** (2012), 181–200. https://doi.org/10.1016/j.jspi.2011.07.007

31. J. Geweke, Evaluating the accuracy of sampling-based approaches to the calculations of posterior moments, *Bayesian Stat.*, **4** (1992), 641–649. https://doi.org/10.1093/oso/9780198522669.003.0010

32. A. E. Raftery, S. M. Lewis, The number of iterations, convergence diagnostics and generic metropolis algorithms, *Pract. Markov Chain Monte Carlo*, **7** (1995), 763–773.

33. J. P. LeSage, *Applied econometrics using MATLAB*, Technical report, Department of Economics, University of Toronto, 1999.

34. C. P. Robert, G. Casella, The metropolis—hastings algorithm, in *Monte Carlo Stat. Methods*. Springer, 2004, 267–320. https://doi.org/10.1007/978-1-4757-4145-2_7

35. W. A. Link, M. J. Eaton, On thinning of chains in mcmc, *Methods Ecol. Evol.*, **3** (2012), 112–115. https://doi.org/10.1111/j.2041-210X.2011.00131.x

36. B. Carpenter, A. Gelman, M. D. Hoffman, D. Lee, B. Goodrich, M. Betancourt, et al., Stan: A probabilistic programming language, *J. Stat. Softw.*, **76** (2017), 1–32.

37. O. Abril-Pla, V. Andreani, C. Carroll, L. Dong, C. J. Fonnesbeck, M. Kochurov, et al., Pymc: A modern, and comprehensive probabilistic programming framework in python, *PeerJ Comput. Sci.*, **9** (2023), e1516.

38. A. Gelman, W. R. Gilks, G. O. Roberts, Weak convergence and optimal scaling of random walk metropolis algorithms, *Ann. Appl. Probab.*, **7** (1997), 110–120.

39. J. W. Taylor, Short-term electricity demand forecasting using double seasonal exponential smoothing, *J. Oper. Res. Soc.*, **54** (2003), 799–805, https://doi.org/10.1057/palgrave.jors.2601589

40. G. Schwarz, Estimating the dimension of a model, *Ann. Stat.*, **6** (1978), 461–464. https://doi.org/10.1214/aos/1176344136

41. D. J. Spiegelhalter, N. G. Best, B. P. Carlin, A. Van Der Linde, Bayesian measures of model complexity and fit, *J. R. Stat. Soc. Ser. B Stat. Methodol.*, **64** (2002), 583–639.

42. J. Geweke, Bayesian treatment of the independent student-t linear model, *J. Appl. Econom.*, **8** (1993), S19–S40. https://doi.org/10.1002/jae.3950080504